

Piotr PORWIK<sup>1</sup>, Maciej SOSNOWSKI<sup>2</sup>, Krzysztof WRÓBEL<sup>1</sup>, Tomasz WESOŁOWSKI<sup>1</sup>

## THE ATTEMPT OF THE BLOOD VESSEL CONTRACTIBILITY ESTIMATION ON THE BASIS OF THE COMPUTED TOMOGRAPHY IMAGING<sup>3</sup>

Cardiovascular mortality remains a leading health and social problem in many countries throughout the world. Its main cause is related to atherosclerosis of coronary and cerebral vessels with their most severe consequences: heart attack and stroke. Therefore, it is obvious that current preventive measures include early detection of atherosclerosis process. Multi-detector computed tomography (MDCT) is one of imaging modalities allowing for noninvasive detection of atherosclerotic lesion within coronary arteries in subjects with accumulation of risk factors (smoking, high lipids, hypertension, male gender, family history) or with suspicion of coronary artery disease (CAD). In is very important that the tomographic images are taken in synchronization with cardiac cycle so that, during few heartbeats, an appropriate series of images can be recorded. Commonly, cardiac MDCT is used for visualization of cardiac and vessels morphology. Heart function can also be determined, however, this MDCT potential is only rarely applied, as current echocardiographic modalities are sufficient. Functional analysis of coronary arteries (flow, reserve) is usually approached by means of invasive procedures. We aimed at finding solution for evaluation of another kind of functional analysis of coronary arteries, namely vessel's wall compliance by means of MDCT coronary angiography.

Under the proposed procedure, on basis of serial CT images of the vessels over entire cardiac cycles, the internal area of the blood vessel is measured and its changes during various phases of heartbeat (systole, diastole) are calculated. If the vessel wall has been changed by atherosclerotic plaque, either calcified or non-calcified, then its compliance will be reduced due to its stiffness. Calculation of coronary artery compliance requires a series of measurements, which is unreliable and impractical for doing manually.

One component of the method described herein involves the images being converted into binary representations and the Hough Transform then applied. The overall methodology proposed in this paper assists in the preparation of a medical diagnosis.

### 1. INTRODUCTION

Heart attack and stroke are two main reasons of cardiovascular mortality - an epidemic in many countries all over the world. The common reason of these two severe complications is atherosclerosis. The process of atherosclerosis is related with development of so-called plaques within arteries' walls through accumulation of lipids, blood cells, calcium, vascular smooth muscle and fibrous cells. It leads to remodeling of vessels which is characterized by thickening and stiffening of their walls. If the process of atherosclerosis is located within coronary arteries then a disease develops known as coronary artery disease (CAD).

Recent advances in non-invasive imaging of coronary arteries using multi-detector computed tomography (MDCT) allow for early detection of atherosclerotic plaques, either by means of coronary artery calcium scoring (CACS) or by means of CT coronary angiography (CTCA) [10,11]. The CACS is the simplest in vivo method in which a series of non-contrast (native) scans is analyzed semi-automatically. Detection of calcium lesions provides an unambiguous proof for the presence of coronary atherosclerosis. If the CACS is high, the probability of the presence of significant coronary lumen stenosis is also high. Additionally, it is possible to evaluate extension of calcified lesions, as CACS can be determined separately for each main coronary artery as well as for their specific parts (segments). Detection of CACS within all main arteries indicates more advanced CAD.

<sup>1</sup> University of Silesia, Institute of Computer Science, ul. Będzińska 39, 41-200 Sosnowiec, Poland, email: {piotr.porwik, krzysztof.wrobel, tomasz.wesolowski}@us.edu.pl.

<sup>2</sup> Unit of the Noninvasive Cardiovascular Diagnostics, 3rd Division of Cardiology, Medical University of Silesia, Upper Silesian Heart Centre, Katowice, Poland.

<sup>3</sup> This paper is an extended version of an article: A Computational Assessment of a Blood Vessels Compliance: A Procedure Based on Computed Tomography Coronary Angiography, The 6th International Conference HAIS 2011, LNAI 6678 Vol. 1, pp. 428-435.

The CTCA requires that similar scans are obtained after injection of contrast agents. Cardiac images ranging from aortic root to the cardiac apex are acquired during a single breath-hold of 10 second.

The CTCA enables for both coronary artery lumen and walls to be visualized. A lumen stenosis that limit coronary blood flow can be quantified and atherosclerotic plaques, both calcified and non-calcified, can be detected and characterized.

At early stages of atherosclerosis, vascular lesions, being small and non-calcified, cannot be easily detected by means of CTCA, taking into account its limited resolution. However, these small atherosclerotic deposits influence upon arterial all function through its thickening and vessel enlargement (so-called positive remodeling). As arterial lumen, estimated on its cross-sections, is changeable over cardiac cycle due to variable blood flow within coronaries, measurements of vessel's cross-sections might help to evidence an abnormal vessel's wall function, namely a decreased compliance [1,4,5]. A procedure based on this data and approach will be presented in this paper.

CT examinations are non-invasive, but during the procedure patient absorbs a sizeable dose of radiation [8]. Modern CT scanners are so fast that they scan through large sections of the body in just a few seconds. Such speed is beneficial for all patients, and especially for children, the elderly and the critically ill. Still, due to the presence of radiation, the computer workstations used for the processing of the image information are located in a separate room, from where the technologist operates the scanner and monitors the examination.

During the examination, some amount of radiation is absorbed by the patient. For example, a chest x-ray is the most commonly performed diagnostic x-ray examination. The mean dose of radiation absorbed during a standard chest x-ray examination is 0.02 mSv [8]. During a CT examination the patient absorbs 400 times the dose of radiation as delivered in a standard chest x-ray. Therefore CT examinations should be organized very carefully.

## 2. DATA ACQUISITION

During CT procedures only raw-data are recorded. It is from this raw-data that images, for display on a work station, are constructed. By using specialized graphics programs, a radiologist can display images built from this data on their monitors in any of a range of scales, in different views, three-dimensional projections and reconstructions. These projections produce the "tomogram": a two-dimensional image of a section, or slice, through a three-dimensional object.

The cardiac CT scans present images similar to Fig. 1. The radiologist indicates the areas and sections of blood vessels where measurement should be conducted. Fig. 1a presents a CT image upon which a blood vessel examination has been performed. In this picture, different cross-sections along the vessel can be studied. Each cross-section is surrounded by a frame, which has been automatically added by the work-station software. Inside the frame, the shape of the cross-section is then estimated. This examination was performed by a Toshiba Aquilion 64 CT scanner and by the Vitrea2 software (Vital Images Inc.) application at the Unit of the Noninvasive Cardiovascular Diagnostic at the Medical University of Silesia. If the reference points for the measurements have been chosen by the physician, then evaluations will be automatically conducted at these points and at points adjacent to each point, both in front of the point and behind it. Here seven locations before and seven locations after the reference point are studied: fifteen blood vessel cross-sections will be investigated. The cross-sections can be separated by a constant distance; here the step size is 0.5 mm.

Fig. 1b shows the patient's ECG pulse as recorded during the examination. The appropriate phases of the patient's pulse trigger the CT imaging. In practice, ten phases of the ECG, separated by a 10% step, are used to construct the images. Hence, the 10 images  $I_1, I_2, \dots, I_{10}$  can be successively displayed, as depicted in Fig. 1a. As was mentioned, inside every individual image  $I_i$ , fifteen sub-images are included:  $I_i \supset \{I_i^1, I_i^2, \dots, I_i^{15}\}$ ; each sub-image  $I_i^j, i = 1, \dots, 10, j = 1, \dots, 15$  includes one cross-section of the analyzed vessel. In total there are 150 sub-images. Thus, one cross-section can be observed over ten heartbeat phases.

For this paper, due to technical restrictions, the images and the places on these images at which measurements are conducted are too small to be properly displayed. Therefore, in Fig. 2, an exemplary

coronary vessel model has been used. In this model a fragment of the vessel displaying pathological changes (having an inner wall layer with calcification) is included, together with a normal fragment, illustrating the positions at which contractibility studies of the vessel are performed. In the same figure (Fig. 2) the reference point (indicator 0) is presented, along with fourteen additional points -1,...,-7,+1,...,+7, at each of which the vessel's cross-section will be displayed and studied.

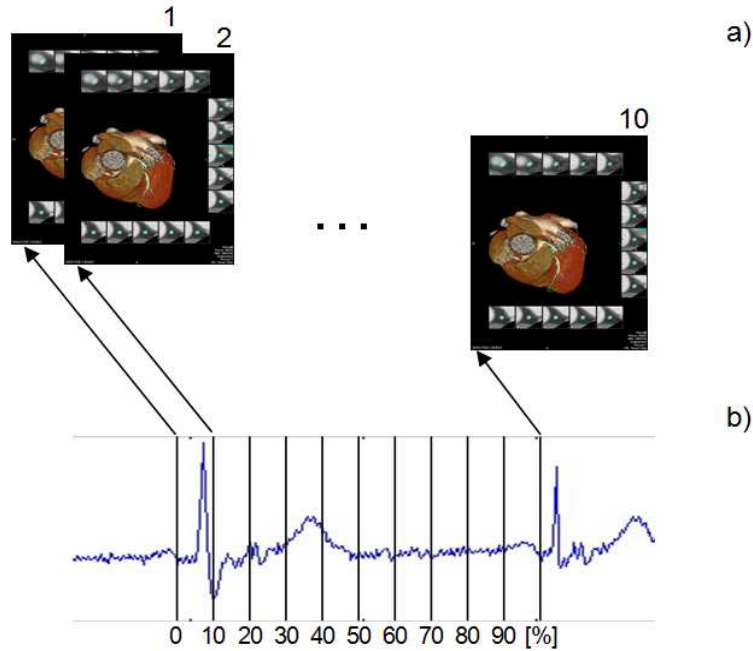


Fig. 1. CT imaging (a), initialized by the ECG strobing signal (b).

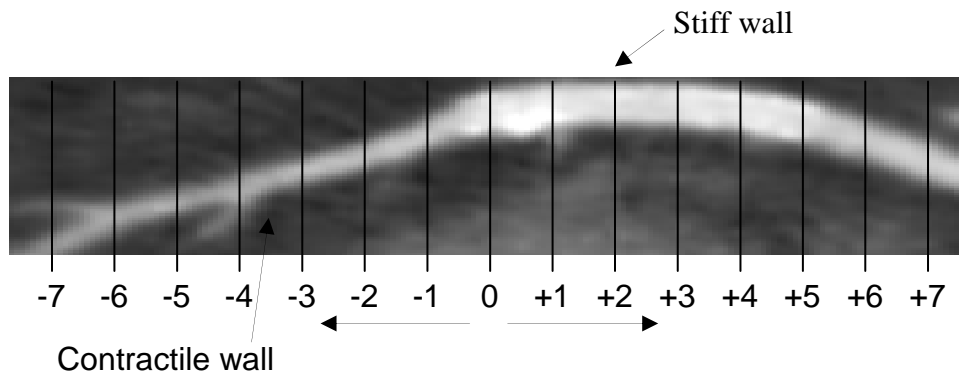


Fig. 2. Exemplary of a pathological coronary vessel sector, with calcified pathological changes (stiff vessel walls), and a normal, contractile vessel's wall. Image was taken from the patient's CT image.

### 3. IMAGE PROCESSING

During the first stage, the appropriate image is constructed, as presented in Fig. 3. This is the image  $I_i$  – the original CT image, using which, the appropriate coronary vessel, as indicated inside the white circle, will be examined by a radiologist. On the same CT image, the 15 frame-sub-images  $I_i^j$  are shown. Each sub-image  $I_i^j$  displays a cross-section of the examined vessel. These cross-sections are automatically selected by the tomograph's controlling software, displayed on the radiologist's computer screen and can then be written to any of a range of graphic formats such as JPG, PNG and many others. These files can each be separately processed by image processing techniques.

In the next stage, the source image is converted into a binary representation, as depicted in Fig. 4a. The CT image is a colour image, with specific set of colours; image  $I$  is presented in an RGB colour space [2,7,9]. The binary representation is established as indicated in the following pseudo-code. Let the current position of the pixel on the image will be denoted by  $I(x, y)$  then:

- binary rule for frame detection:

```

if ((R=178,G=178,B=178) or (R=100,G=149,B=237) or
    (R=0,G=205,B=0) or (R=240,G=128,B=128))
    the pixel  $I(x,y)$  is changed to black (R=G=B=0);
else
    the pixel  $I(x,y)$  is changed to white (R=G=B=255);
endif
    
```

- binary rule for cross-section detection:

```

if ((R>90) or (G<140 or G>240) or (B<80 or B>240))
    the pixel  $I(x,y)$  is changed to white (R=G=B=255);
else
    the pixel  $I(x,y)$  is changed to black (R=G=B=0);
endif
    
```



Fig. 3. The source CT image.

The process of conversion into a binary image permits the extraction of both the frame that surrounds each sub-image, as well as the shapes of the cross-sections inside each frame. After conversion into a binary representation, in the central region of the image (Fig. 4a), some artifacts can be observed. Similar noise inside the frames is also present. It should be noted that in the cross-sections, especially the shapes of these cross-sections, are clearly visible and properly detected, so that these artifacts of the image can be correctly extracted.

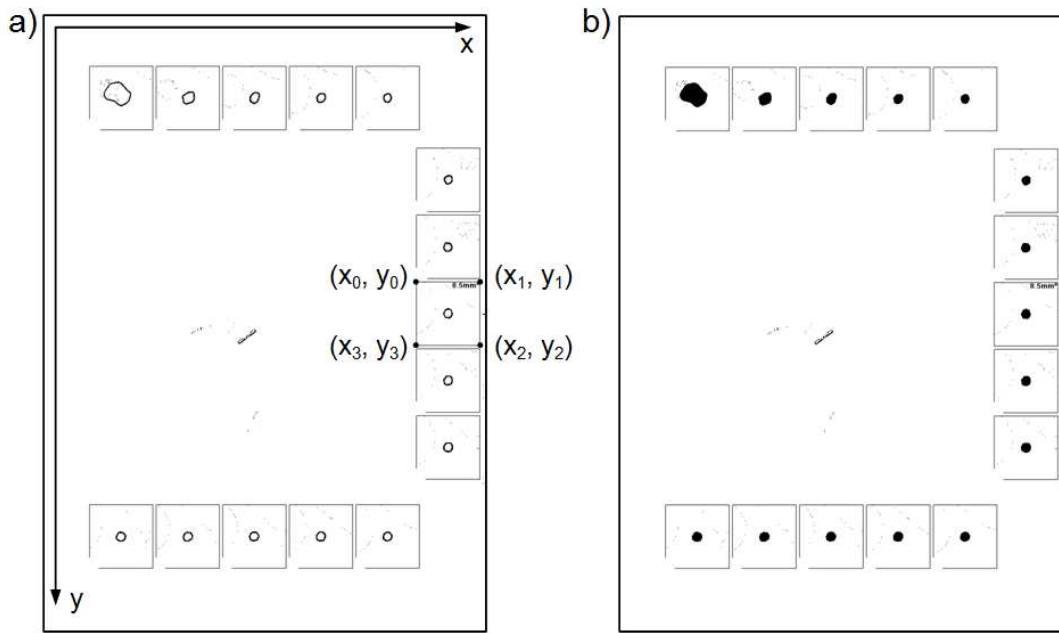


Fig. 4. The CT image after conversion to binary (a), and the same image with filled cross-sectional areas (b).

In the subsequent step, the coordinates of the four vertexes of every frame are established. The vertex coordinates are calculated by using the Hough Transform (HT) [3,6] combined with the algorithm of Binary Image's Contour Parameterization (presented below). In this paper the modified Hough Transform for straight horizontal and vertical lines was applied. This modification of the HT significantly decreased processing time of the source CT image.

The algorithm of Binary Image's Contour Parameterization:

Input data:

1. Binary image of dimension  $H \times W$  (in pixels),
2.  $IL$  – the list of horizontal and vertical lines which have been extracted from image by using the Hough Transform,
3.  $L$  – the minimal length of the section to find (in pixels).

Output data:

1.  $OL$  – the list of appropriate sections found in the whole binary image.

```

for (all lines in  $IL$  list)
  if (line is horizontal)
    create and initialize temporary array  $Tab[0..H]$ ;
    for (every line point  $i$  from 0 to  $H$ )
      if ( $i$  is a black image point)
         $Tab[i] = 1$ ;
      else
         $Tab[i] = 0$ ;
      endif
    endfor
  else // line is vertical
    create and initialize temporary array  $Tab[0..W]$ ;
    for (every line point  $j$  from 0 to  $W$ )
      if ( $j$  is a black image point)
         $Tab[j] = 1$ ;
      else
         $Tab[j] = 0$ ;
      endif
    endfor
  endif
endif
    
```

```
// analyze array Tab
for (all cells of array Tab)
  find series of value 1 of length >= L;
  basing on the first and the last index of the series, calculate begin and end
  coordinates of the section on the image;
  store begin and end coordinates of the section in the OL list;
endfor
endfor
```

If each frame's coordinates are numbered in a clockwise fashion, then the first frame's centre of gravity will have the coordinates  $(x_1', y_1') = \left( \frac{x_1 - x_0}{2}, \frac{y_3 - y_0}{2} \right)$ , and similarly for the points of each following frame. Thus the  $(x_j', y_j')$ ,  $j=1, \dots, 15$  points are fixed. Now each cross-section is centered to its point  $(x_j', y_j')$ . The reference frame, selected by the physician, includes a cross-sectional area (in  $\text{mm}^2$ ), automatically computed by the tomograph's controlling software. Obviously, the CT images are taken with a uniform resolution. Thus there are a fixed number of pixels inside each cross-section's perimeter. In each successive step, the area of the cross-section is filled with black pixels (Fig. 4b) and the number of pixels inside the remaining cross-sections is assigned. Hence, by a simple computation the remaining cross-sectional areas,  $\text{mm}^2$ , can be determined. Currently, a diagnosis of atherosclerosis disease can be made when  $1\text{mm}^2$  or more of the vessel's cross-sectional area is occupied by atherosclerotic plaque.

#### 4. THE RESULTS OBTAINED

The determination of the contractibility of coronary vessels has been practically demonstrated for sets of images derived from three patients. Each image consisted of a set of 15 sub-images, as shown in Fig. 4. These images were processed by the image processing procedures described in the previous paragraphs. The two outermost cross-sections (+7, +6 and -7, -6) were not analyzed because, during the observation, the physician could not accurately identify the reference cross-section, the 0 point. Additionally, the extreme points can be closer to vessel branching points. Hence, only eleven of the vessel cross-sections have been examined. The vessel cross-section changes across the ten phases (T%) of the cardiac cycle have been listed (see Table 1). Table 1 includes the complete results from the measurements made on one patient.

Table 1. Vessel cross-sectional changes across the ten phases of the cardiac cycle. Data of the one patient.

|          | The vessel's cross-sections [ $\text{mm}^2$ ] |       |       |       |       |       |       |       |       |       |       |
|----------|---|-------|-------|-------|-------|-------|-------|-------|-------|-------|-------|
| T [%]    | 5   | 4     | 3     | 2     | 1     | 0     | -1    | -2    | -3    | -4    | -5    |
| 0        | 7,93  | 8,06  | 7,90  | 8,43  | 8,50  | 8,40  | 8,94  | 8,94  | 9,17  | 9,17  | 10,08 |
| 10       | 8,63  | 9,39  | 10,71 | 12,21 | 14,62 | 15,90 | 17,69 | 16,81 | 13,78 | 8,99  | 8,08  |
| 20       | 9,90  | 9,34  | 9,55  | 9,21  | 9,17  | 9,90  | 10,63 | 10,49 | 10,70 | 10,46 | 12,12 |
| 30       | 8,93  | 8,79  | 9,55  | 9,17  | 9,31  | 10,00 | 10,83 | 10,38 | 11,17 | 11,14 | 12,07 |
| 40       | 6,72  | 6,93  | 7,28  | 8,34  | 9,97  | 11,00 | 12,14 | 12,48 | 13,59 | 14,59 | 14,93 |
| 50       | 7,31  | 6,89  | 5,88  | 6,48  | 6,71  | 6,80  | 6,58  | 7,18  | 7,78  | 7,84  | 9,90  |
| 60       | 16,57   | 12,23 | 9,83  | 8,17  | 7,70  | 7,50  | 7,73  | 7,87  | 8,07  | 8,30  | 8,90  |
| 70       | 10,87   | 8,84  | 7,65  | 7,62  | 8,09  | 8,50  | 8,74  | 9,08  | 8,60  | 9,18  | 9,01  |
| 80       | 7,57  | 7,11  | 6,87  | 7,57  | 8,20  | 8,60  | 8,77  | 8,97  | 8,90  | 9,30  | 9,36  |
| 90       | 7,19  | 7,16  | 7,09  | 8,10  | 8,46  | 9,00  | 8,80  | 9,03  | 9,03  | 9,33  | 9,27  |
| Variance | 7,59  | 2,46  | 2,22  | 2,07  | 4,15  | 5,81  | 8,73  | 6,93  | 4,24  | 3,31  | 3,86  |

The vessel's contractibility was measured by calculating the variance of these measurements. This measure allows for an evaluation of the dynamics of the changes in the vessel's wall. The last row of Table 1 lists the variance in the vessel's cross-sectional areas. In the table it can be seen that the greatest contractibility of the vessel is in cross-section number -1, and the least contractibility is in cross-section

number 2. Where the dynamics of the vessel wall are small pathological changes can occur, especially changes that anticipate atherosclerotic plaque.

The results gathered in Table 1 can be presented more conveniently, that is graphically. See Fig. 5 and Fig. 6.

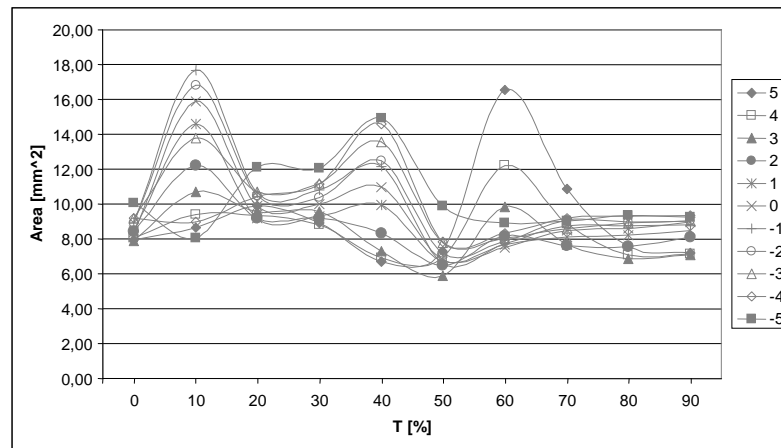


Fig. 5. Vessel cross-sectional areas, by phase of the cardiac cycle.

A similar graphic projection was depicted on Fig. 6, where the changes in vessel cross-sectional areas over the cardiac cycle are depicted, by section.

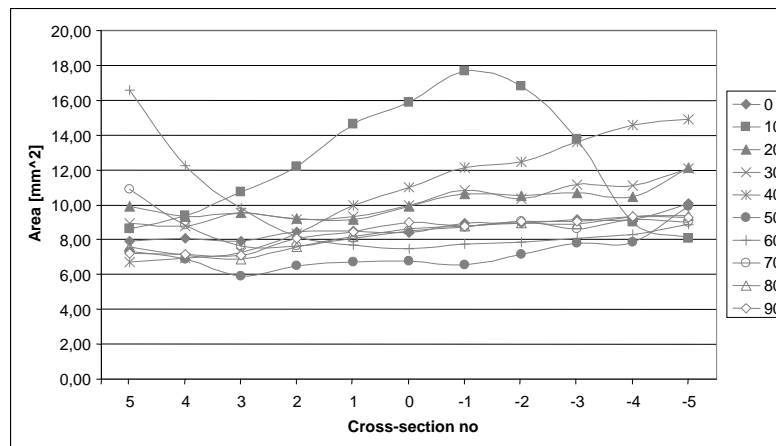


Fig. 6. Changes in blood vessel cross-sectional area, by section.

From the data displayed in Fig. 5 and Fig. 6 it can be noticed that the vessel has good contractibility during all phases of the cardiac cycle so, with high degree of probability, atherosclerosis disease is not present in the vessel examined. For comparison, in Table 2, data is presented from a patient that has been diagnosed as having atherosclerotic plaque.

Table 2. Variance of coronary vessel cross-sectional areas. Data of a patient with atherosclerotic plaque.

|          | Number of cross-section |      |      |      |      |      |      |      |      |      |      |
|----------|-------------------------|------|------|------|------|------|------|------|------|------|------|
|          | 5                       | 4    | 3    | 2    | 1    | 0    | -1   | -2   | -3   | -4   | -5   |
| Variance | 7,59                    | 2,48 | 2,22 | 0,18 | 2,57 | 2,89 | 4,45 | 5,08 | 4,24 | 3,34 | 2,90 |

From Table 2 it can be clearly seen that cross-section number 2 has a very small contractibility, indicating a risk of disease. As with the previous example, the full data can be presented graphically (Fig. 7 and Fig. 8).

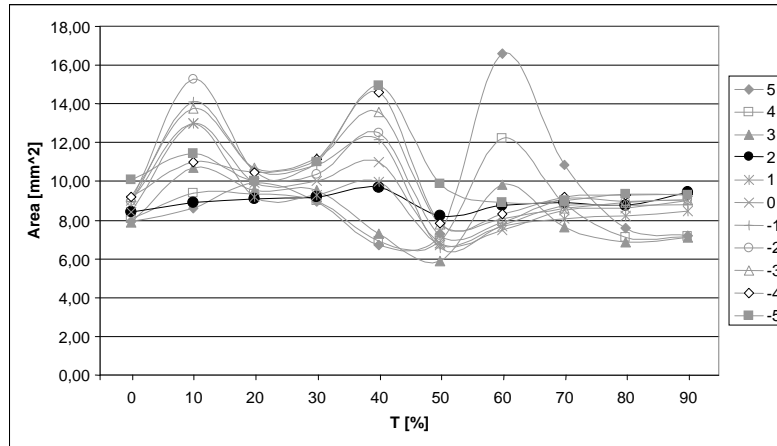


Fig. 7. Vessel cross-sectional areas across the cardiac cycle, from a patient with atherosclerotic plaque.

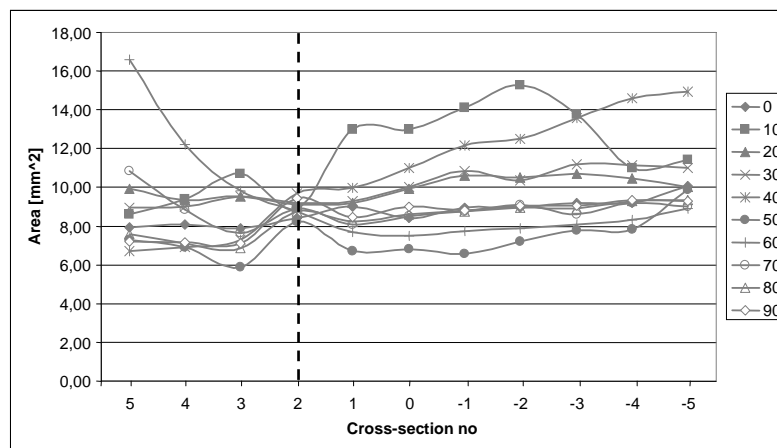


Fig. 8. Changes in blood vessel cross-sectional area, by section, from a patient with atherosclerotic plaque.

In Fig. 7 and Fig. 8 it can be clearly seen that the coronary vessel's cross-section number 2 is almost constant throughout the cardiac cycle. This location is, probably, already calcified as the vessel wall has become stiffened.

If inner layer of the artery is calcified, but pathological changes are still small, then these pathologies cannot be imaged by normal CT procedures. However, pathologies of this type can be observed by the method described in this paper. This approach can also be used for automatic cross-sectional area computation in cases when pathological changes inside vessel are already well visible on CT images.

## 5. CONCLUSIONS

The method proposed in this paper allows for data to be automatically read from CT images. Some additional information can also be extracted from these images. This additional information has been credibly and correctly interpreted, and the interpretation given matched the diagnosis made by a physician during the patient's examination.

The CT dataset derive from the Medical University of Silesia archives and from current medical examinations. All these images are owned by the Medical Centre. During investigations 30 CT images have been transformed and then processed, according to the presented in this paper method. This procedure – as our software – is used by physicians during CT image analysis.

The procedure detailed herein was accomplished with a graphical C# program tool that runs on all tomography workstations. Thus, using this new technique, CT images can be also studied at medical centres at which computed tomography is not present. This is possible as, after their examination, the patient can obtain their data and medical documentation on CD media. It should be emphasized here that this method permits the identification of pathological changes when these changes are not yet visible on CT images.

#### BIBLIOGRAPHY

- [1] CHIEN C., FENG YF., ARORA RR., Advances in computed tomography-based evaluation of coronary arteries: a review of coronary artery imaging with multidetector spiral computed tomography, *Rev. Cardiovasc. Med.* Vol. 8, 2007, pp. 53-60.
- [2] DOUGHERTY G., *Digital Image Processing for Medical Applications*, Cambridge University Press, 2009.
- [3] DUDA R.O., HART P.E., Use of Hough transformation to detect lines and curve in pictures, *Comm. ACM*, Vol. 15, 1972, pp. 11-15.
- [4] GOLA A., PYSZ P., SZYMANSKI L., SOSNOWSKI M., TENDERA M., Has MSCT became a reliable tool to evaluate the coronary artery lumen yet? *Eur Radiol.*, Vol. 17, 2007 (abstract).
- [5] GOLA A., PYSZ P., SZYMANSKI L., SOSNOWSKI M., 64-slice MDCT coronary artery functional assessment in zero calcium score patients – a novel parameter emerging, *Eur. Radiol.* Vol. 18 (supl.3): C25 (86), 2008.
- [6] HOUGH P.V.C., Method and Means for recognizing complex pattern, U.S. Patent No. 3069654, 1962.
- [7] KINDRATENKO V., *Development and Application of Image Analysis Techniques for Identification and Classification of Microscopic Particles*, PhD. Thesis, Antwerpen, 1997.
- [8] METTLER F., HUDA W., YOSHIZUMI T., MAHESH M., *Effective Doses in Radiology and Diagnostic Nuclear Medicine: A Catalog*, Radiology, Vol. 248, No. 1, 2008, pp. 254-263.
- [9] NIXON M.S., AGUADO A.S., *Feature Extraction and Image Processing*, Second Edition, Academic Press, Elsevier Ltd., 2008.
- [10] SCHROEDER S., KOPP A.F., BAUMBACH A., et al., Noninvasive detection and evaluation of atherosclerotic coronary plaques with multislice computed tomography, *J.Am.Coll.Cardiol.* Vol. 37, pp. 1430-5, 2001.
- [11] WALECKI J., SOSNOWSKI M., ZAWADZKI M., Tomografia komputerowa serca. In: *Kardiologia. Szczeklik A., Tendera M. (eds), Medycyna Praktyczna Kraków*, 2009, pp. 130-142, (in Polish).

